Photophysical Properties of Pyrene in Zeolites: Adsorption and Distribution of Pyrene Molecules on the Surfaces of Zeolite L and Mordenite

Xinsheng Liu and J. Kerry Thomas*

Department of Chemistry and Biochemistry, University of Notre Dame, Notre Dame, Indiana 46556

Received April 4, 1994. Revised Manuscript Received August 18, 1994®

Adsorption of pyrene on the surfaces of zeolites L and mordenite is investigated using photophysical techniques. Although the internal surfaces of both zeolites are polar, their external surfaces may not be the same. A difference is observed for mordenite. No pyrene excimers can be produced in mordenite, while excimers are readily formed in zeolite L. Due to structural constraints, 30–35% of pyrene adsorbed in mordenite cannot be quenched by O_2. Rotational movement of pyrene molecules in mordenite is also restricted by the zeolite structure. Laser photolysis produces pyrene cation and anion radicals, the former having a larger yield than the latter in both zeolites.

Introduction

Zeolites, due to their unique structural and physicochemical properties, have been consistently used in a technical sense in many fields such as adsorption, separation, catalysis, and wastewater treatment.[1–5] A number of reports on the marked effects of constraints placed by zeolites on various photophysical and photochemical processes such as radical recombination, charge stabilization, and energy and electron transfers have been published recently.[6–12] Several studies of photophysical properties of pyrene in zeolites such as X and Y have been reported.[8,12] These studies involve surface polarity, excimer formation, oxygen quenching of excited pyrene, energy transfer between the adsorbed arene molecules, and electron transfer between metal cations and pyrene molecules. The effects of co-adsorbed water and solvent on these events have also been studied.[12b,e,13,14] In this paper, results are presented of a study of zeolites, zeolite L, and mordenite, using pyrene as a probe molecule. Zeolite L and mordenite have channel structures which are different from the cage structures of zeolites X and Y and have technological applications in separation processes and catalysis.[5] The results presented provide fundamental insight into the adsorption and distribution of pyrene molecules in these samples, properties that pertain to their industrial usage.

Experimental Section

Zeolites and Chemicals. Na^+-mordenite with a composition (dehydrated) of $Na_{7.6}Al_{7.6}Si_{40.4}O_{96}$ (Si/Al = 5.3) was kindly provided by UOP. K^+-zeolite L was hydrothermally synthesized following the gel composition given in Breck's book[1] and characterized using X-ray diffraction, electron microscopy and wet chemical analysis.[15] The characterization confirmed that the zeolite L synthesized was of high purity and had a composition of $K_{8.8}Al_{8.8}Si_{27.2}O_{72}$ (Si/Al = 3.1). Pyrene (99+%) and *n*-pentane (99+%) were from Aldrich. Pyrene was purified by silica gel/cyclohexane column chromatography, followed by recrystallization from cyclohexane. *n*-Pentane was stringently dried with activated molecular sieve 3A pellets.

Sample Preparation. Zeolites L and mordenite, after being dehydrated at 330 °C overnight, were suspended in liquid *n*-pentane in vials, and a solution of pyrene was added. The vials were sealed, shaken, and then stored in the dark overnight. The solid was separated by filtration and washed with *n*-pentane, and the supernatant was collected for analysis. The amount of pyrene adsorbed on the zeolites was calculated by subtraction of the residual in the supernatant from the total amount of pyrene in the solution. Samples were immediately transferred into quartz tubes or cuvettes and evacuated to a pressure of 1×10^{-3} Torr.

Instruments. Steady-state emission and excitation spectra were measured on a SLM SPE 500C fluorimeter equipped with a 250 W xenon arc lamp. The fluorescence anisotropy mea-

* To whom correspondence should be addressed.

® Abstract published in *Advance ACS Abstracts,* October 15, 1994.

(1) Breck, D. W. *Zeolite Molecular Sieves*; Wiley: New York, 1974.
(2) Katzer, J. R., Ed. *Molecular Sieves II*; ACS Symposium Series 40, 1977.
(3) Rabo, J. A., Ed. *Zeolite Chemistry and Catalysis*; ACS Monographs 171, 1976.
(4) Bhatia, S. *Zeolite catalysis: Principles and applications*; CRC Press: Boca Raton, FL,1989.
(5) Van Bekkum, H., Flanigen, E. M., Jansen, J. C., Eds. *Introduction to Zeolite Science and Practice*; Elsevier: Amsterdam, 1991.
(6) (a) Baretz, B. H.; Turro, N. J. *J. Photochem.* **1984**, *24*, 201. (b) Turro, N. J. *Photochemistry in Organized and Constrained Media*; Ramamurthy, V., Ed.; VCH Publishers: New York, 1991; p 1.
(7) Kevan, L. *Rev. Chem. Intermed.* **1987**, *8*, 53–58.
(8) (a) Ramamurthy, V.; Caspar, J. V.; Corbin, D. R. *J. Phys. Chem.* **1990**, *94*, 3391. (b) Ramamurthy, V. *Photochemistry in Organized and Constrained Media*; Ramamurthy, V., Ed.; VCH Publishers: New York, 1991; p 429. (c) Ramamurthy, V.; Eaton, D. F.; Caspar, J. V. *Acc. Chem. Res.* **1992**, *25*, 299.
(9) (a) Casal, H. L.; Scaiano, J. C. *Can. J. Chem.* **1985**, *63*, 1308. (b) Wilkinson, F.; Willsher, C. J.; Casal, H. L.; Johnston, L.; Scaiano, J. C. *Can. J. Chem.* **1986**, *64*, 539. (c) Kelley, G.; Willsher, C. J.; Wilkinson, F.; Netto-Ferreira, J. C.; Olea, A.; Weir, D.; Johnston, L. J.; Scaiano, J. C. *Can. J. Chem.* **1990**, *68*, 812.
(10) (a) Yoon, K. B.; Kochi, J. K. *J. Am. Chem. Soc.* **1989**, *111*, 1128. (b) Yoon, K. B.; Kochi, J. K. *J. Phys. Chem.* **1991**, *95*, 3780. (c) Sankararaman, S.; Yoon, K. B.; Yabe, T.; Kochi, J. K. *J. Am. Chem. Soc.* **1991**, *113*, 1419.
(11) Kim, Y. I.; Mallouk, T. E. *J. Phys. Chem.* **1992**, *96*, 2879.
(12) (a) Liu, X; Iu, K.-K.; Thomas, J. K. *J. Phys. Chem.* **1989**, *93*, 4120. (b) Iu, K.-K.; Thomas, J. K. *Langmuir* **1990**, *6*, 471. (c) Iu, K.-K.; Thomas, J. K. *J. Phys. Chem.* **1991**, *95*, 506. (d) Iu, K.-K.; Liu, X.; Thomas, J. K. *Mater. Res. Soc., Symp. Proc.* 233; 1991; p 119. (e) Iu, K.-K.; Thomas, J. K. *Colloids* **1992**, *63*, 39.
(13) Dinesenko, G. I. *Zh. Prikl. Spektrosk.* **1968**, *9*, 307.
(14) Incavo, J. A.; Dutta, P. K. *J. Phys. Chem.* **1990**, *94*, 3075.
(15) Xu, R.; Liu, X. *Acta Chim. Sin.* **1984**, *42*, 227.

0897-4756/94/2806-2303$04.50/0

Table 1. Adsorption and Existing State of Pyrene in Zeolite L and Mordenite with Different Pyrene Loadings

no.	zeolite	concentration of pyrene mol/g	concentration of pyrene $N_{py/u.c.}$	state of pyrene	% adsorbed from solution
1	K–L	9.315×10^{-7}	0.0023	monomer	>99.9
2	K–L	1.349×10^{-6}	0.0034	monomer + excimer	>99.9
3	K–L	2.294×10^{-6}	0.0057	monomer + excimer	>99.9
4	K–L	2.694×10^{-6}	0.0067	monomer + excimer	>99.9
5	K–L	3.402×10^{-6}	0.0085	monomer + excimer	>99.9
6	K–L	4.901×10^{-6}	0.0123	monomer + excimer	>99.9
7	Na–M	5.854×10^{-7}	0.0018	monomer	87.4
8	Na–M	9.512×10^{-7}	0.0029	monomer	85.0
9	Na–M	1.030×10^{-6}	0.0031	monomer	83.1
10	Na–M	1.972×10^{-6}	0.0060	monomer	76.2
11	Na–M	2.443×10^{-6}	0.0074	monomer	73.8
12	Na–M	3.771×10^{-6}	0.0115	monomer	64.7
13	Na–M	3.995×10^{-6}	0.0122	monomer	64.3

surements were performed also on the same instrument with the polarizers separately located in the excitation and emission beams. The angle between the surface of cuvette and the excitation light was set to 30° in order to avoid the reflected light to be detected by the detector. Time-resolved laser spectroscopic studies were carried out as described in previous publications.[12a,e]

Results and Discussion

Adsorption of Pyrene. Table 1 gives adsorption data of pyrene on zeolite L and mordenite. Over the range of pyrene concentration studied, zeolite L adsorbs all pyrene molecules from the *n*-pentane solution (>99.9%), while mordenite adsorbs only a portion of them (see Table 1). The amount of pyrene adsorbed by mordenite increases with increasing pyrene concentration, but the percentage of pyrene molecules adsorbed decreases.

Figure 1 shows steady-state emission spectra of pyrene in zeolite L and mordenite with different pyrene loadings. The spectra illustrate several features of pyrene in these zeolites: (1) The zero–zero fluorescence transition at 372 nm is very prominent compared to later transitions. This is indicative of a polar environment for pyrene in both zeolite channels.[8,12] (2) Low pyrene loadings give only the monomer emission in both zeolites, but when the pyrene loading is larger than 1×10^{-6} mol/g, pyrene excimers are produced on zeolite L. Pyrene excimers are never observed on mordenite even at a pyrene concentration as high as 4×10^{-6} mol/g. At these concentrations, a significant amount of pyrene is left in the supernatant (see Table 1).

The zeolite surface can be divided into two categories: internal and external surfaces. The internal surface is the surface inside the channels, while the external surface is mainly the boundary of microcrystals. For adsorption on these surfaces, the internal surface is constrained by the entry aperture of the channel, but the external surface is free for guest molecules to reach. The adsorption behavior observed for zeolite L and mordenite is reminiscent of the adsorption of pyrene on surfaces of solids such as silica, alumina, and clays. In these cases, the adsorption of pyrene is known to be dependent on the surface hydrophilicity,[16–18] and removal of surface OH groups

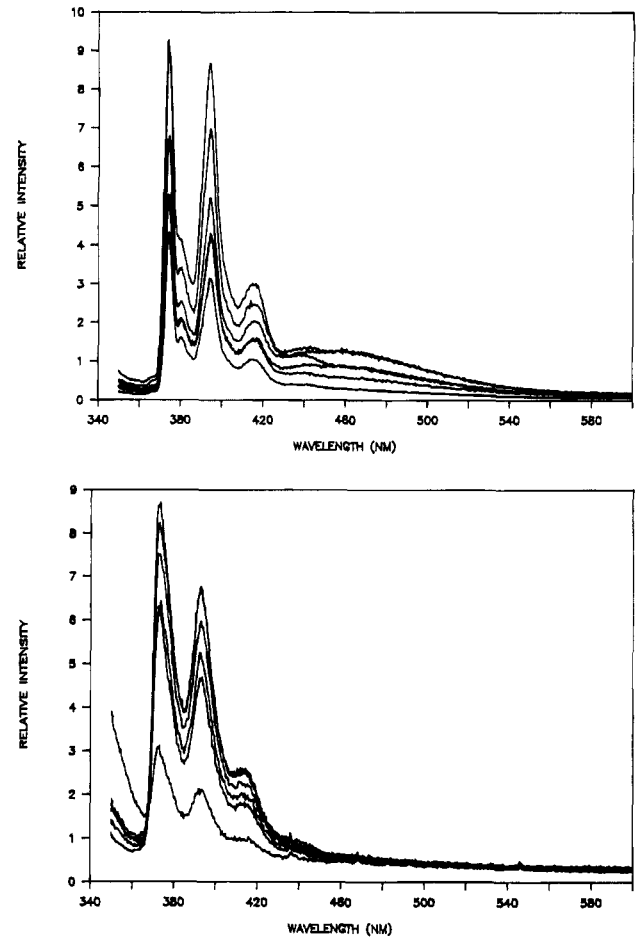

Figure 1. Steady-state fluorescence spectra of pyrene in zeolite L (a) and mordenite (b) with different pyrene loadings. Concentration of pyrene increases from bottom spectrum to top spectrum; see Table 1 for details.

reduces or eliminates adsorption of pyrene to the surface. The phenomena observed therefore indicate that the internal and external surfaces of zeolite L are both hydrophilic and adsorb pyrene molecules, while those of mordenite are significantly different, the internal surface being polar as seen from the pyrene emission spectra, the external surface being less polar and not adsorbing pyrene molecules as with zeolite L. This difference is probably due to the high Si/Al ratio of mordenite and to the different distribution of Si and Al in the bulk and on the external surface of the particles of mordenite.[19] More studies serve to illustrate the marked differences that pyrene experiences in these two zeolites.

Location of Pyrene Excimers. At high pyrene loadings, excimers are readily formed on zeolite L (see Table 1). The location of pyrene excimers, inside the channels or on the external surface, depends on the pore size of the zeolite. For both zeolite L and mordenite, the pyrene monomer could penetrate into the channels without difficulty, but if the excimers are present in the form of ground-state "dimers", they are expected to be

(16) (a) Krasnansky, R.; Koike, K.; Thomas, J. K. *J. Phys. Chem.* **1990**, *94*, 4521. (b) Hite, P.; Krasnansky, R.; Thomas, J. K. *J. Phys. Chem.* **1986**, *90*, 5765.

(17) (a) Pankasem, S.; Thomas, J. K. *J. Phys. Chem.* **1990**, *94*, 4521. (b) Pankasem, S.; Thomas, J. K. *J. Phys. Chem.* **1991**, *95* , 6990.

(18) (a) Liu, X.; Thomas, J. K. *Langmuir* **1991**, *7*, 2808. (b) Iu, K.-K.; Liu, X.; Thomas J. K. *Chem. Phys. Lett.* **1991**, *182*, 531. (c) Liu, X.; Iu, K.-K.; Thomas, J. K. *Langmuir* **1992**, *8*, 539.

(19) Tempere, J. F.; Delafosse, D.; Contour, J. P. *Chem. Phys. Lett.* **1975**, *33*, 95.

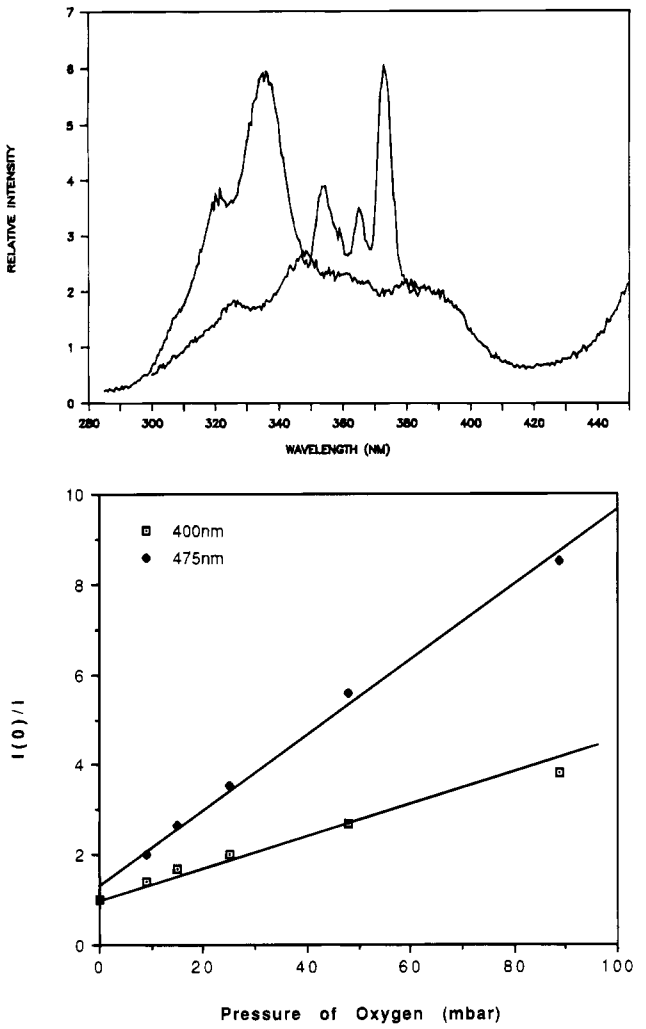

Figure 2. (a) Excitation spectra of pyrene in zeolite L monitored at 400 nm (top) and 465 nm (bottom). Pyrene loading, 4×10^{-6} mol/g. (b) Stern–Volmer plots of oxygen quenching for Py* monomer and excimer in zeolite L with high pyrene loading, 4×10^{-6} mol/g. The monitored wavelengths are given in the figure.

located only on the external surfaces. It is known that a hydrophilic external surface of zeolites such as zeolite A[12a] favors formation of ground-state pyrene "dimers".

Excitation spectroscopic studies of pyrene–zeolite L (Py–zeolite L) with a high pyrene loading support the above speculation. The excitation spectra, given in Figure 2a, of Py–zeolite L monitored at 400 nm for pyrene monomer and 465 nm for pyrene excimer, demonstrate that the nature of the excimer is a ground-state "dimer". The significant spectral shift toward lower energy for the excimer exhibits a characteristic spectrum of ground-state pyrene "dimers" observed in the systems such as γ-cyclodextrin[20,21] and zeolites X and Y.[12a] Steady-state fluorescence quenching of Py* in Py–zeolite L by O_2 provides evidence for the location of the pyrene dimers. Figure 2b shows the Stern–Volmer plots of the O_2 quenching studies. The O_2 quenching is more efficient for pyrene excimer ($k_q = 1.54 \times 10^6$ s^{-1} mbar^{-1}) than for pyrene monomer ($k_q = 7.62 \times 10^5$ s^{-1} mbar^{-1}), in contrast to that observed for Py–

(20) Yorozu, T.; Hoshimo, M.; Imamura, M. *J. Phys. Chem.* **1982**, *86*, 4426.
(21) Zagrobelny, J.; Betts, T. A.; Bright, F. V. *J. Am Chem. Soc.* **1992**, *114*, 5249.

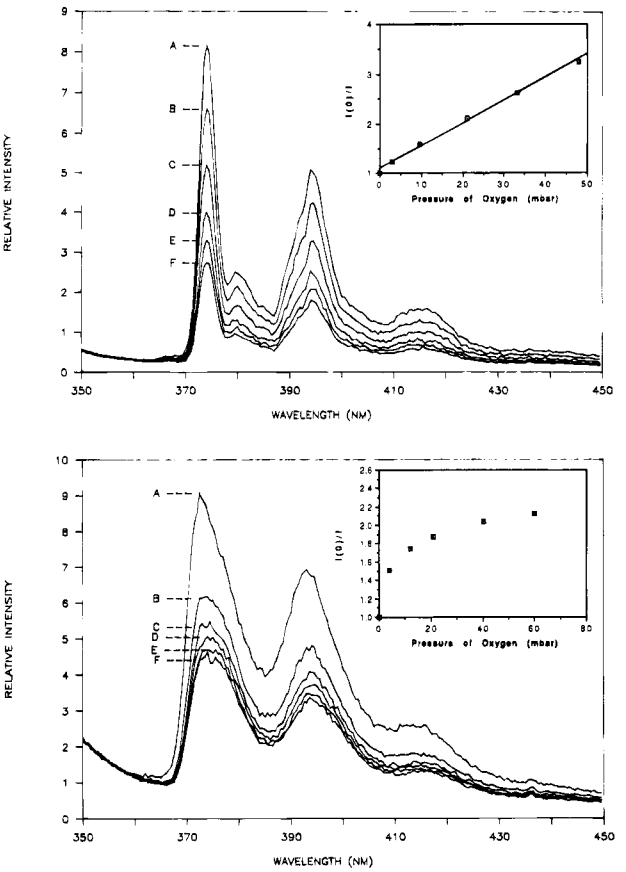

Figure 3. . Steady-state O_2 quenching of pyrene fluorescence for Py–zeolite L (a) and Py–mordenite (b) with a low loading (8×10^{-7} mol/g) and their corresponding Stern–Volmer plots (inserts). O_2 pressure (mbar) for Py–zeolite L from A to F is 0, 3, 9.5, 21, 32, and 48, respectively, and for Py–mordenite from A to F is 0, 4, 12, 21, 40, and 60.

zeolites X and Y where the pyrene "dimers" are located inside the supercages.[12a]

It is also noted that the k_q value for the excited pyrene monomer is independent on the pyrene concentration (see below). The same value was obtained for the samples with different pyrene loadings. This provides further evidence for the different location of excited pyrene monomers and excimers (internal versus external surfaces) in the sample and indicates that the channel structure of the zeolite exclusively prevents the formation of pyrene excimers inside the channels as the concentration increases. In the case of mordenite where the excimer cannot be formed on its external surface, the same decay rate of Py* was always observed for the samples with different pyrene loadings.

Accessibility of Pyrene Molecules. Figure 3 shows steady-state O_2 quenching of pyrene fluorescence for Py–zeolite L and mordenite with a low pyrene loading (i.e., in the absence of pyrene dimers) and their corresponding Stern–Volmer plots (inserts). For Py–zeolite L, the plot is linear (insert in Figure 3a), while for Py–mordenite, a curved line is obtained (insert in Figure 3b). From the slope of the straight line together with the lifetime measurements, the O_2-quenching rate constant (k_q) for Py–zeolite L is estimated to be 7.43×10^5 s^{-1} mbar^{-1}. For Py–mordenite, however, the k_q cannot be obtained from the Stern–Volmer plot as it is not linear. The curvature in the Stern–Volmer plot for O_2 quenching of pyrene fluorescence in the Py–morden-

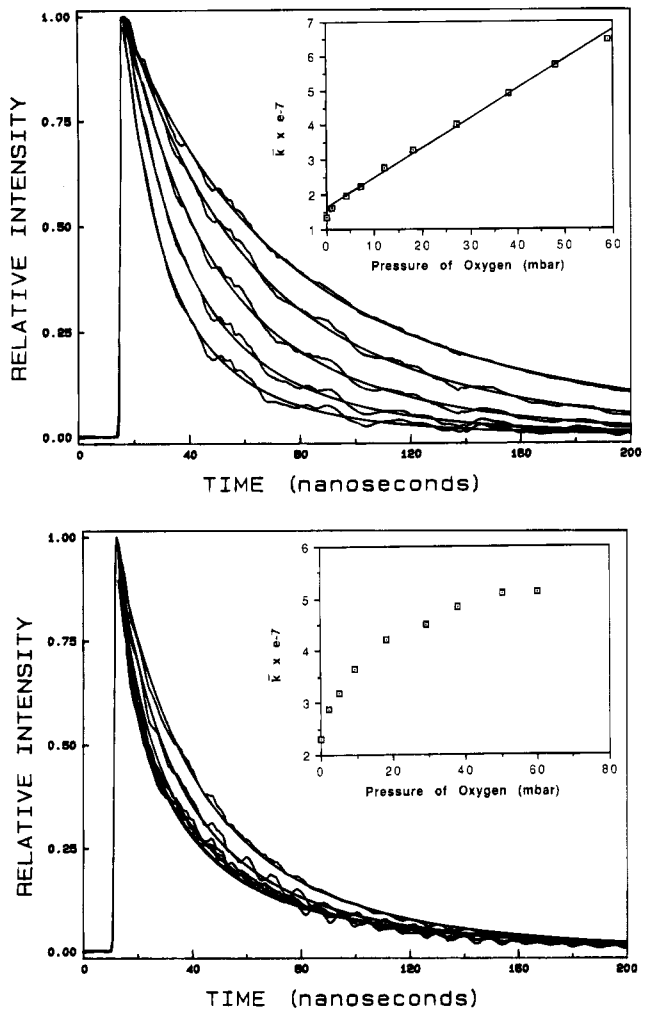

Figure 4. Time-resolved emission decay and O_2 quenching of Py–zeolite L (a) and Py–mordenite (b). Pyrene loading, 8 × 10^{-7} mol/g. The decay curves for Py–zeolite L under O_2 pressures 0, 1, 7, 18, and 38 mbar, and those for Py–mordenite under O_2 pressures 0, 2, 9.5, 29, and 50 mbar are shown. Inserts: relationship between the observed decay rate constant, $\bar{k}_0$, and the O_2 pressure.

ite system results from the inaccessibility of some pyrene molecules in the sample to O_2. The pyrene molecules near the channel entry prevent O_2 molecules from diffusing to pyrene molecules further inside the channel. The proportion of the unquenchable pyrene in mordenite with different pyrene loadings (samples 9, 11, and 13 in Table 1) is estimated from steady-state O_2 quenching studies to be 30–35% of the total pyrene amount in the samples.

Studies of time-resolved emission decay and O_2 quenching of both samples (Figure 4) reveal that the emission decays of Py* in the zeolites follow not a single exponential but a Gaussian distribution kinetics. The Gaussian distribution kinetic model was developed by Albery et al. on the basis of an energetic consideration[22] and subsequently has been successfully applied to the time-resolved fluorescence studies of aromatic molecules on silica,[16] TiO_2,[23] alumina,[17] clays,[18] zeolites,[24] and anionic molecular assembly environments.[25] According

Table 2. Data from O_2 Quenching of Emission of Pyrene* in Zeolite L and Mordenite Fitted with the Gaussian Distribution Model

zeolite L			mordenite		
pressure of O_2 (mbar)	$\bar{k}_{obs}$ ($\times 10^{-7}$)[a]	γ	pressure of O_2 (mbar)	$\bar{k}_{obs}$ ($\times 10^{-7}$)[a]	γ
0	1.37	0.60	0	2.30	0.86
1	1.63	0.72	2	2.88	0.77
4	1.96	0.68	5	3.18	0.84
7	2.25	0.68	9.5	3.65	0.97
12	2.77	0.74	18	4.21	1.10
18	3.30	0.75	29	4.50	1.21
27	4.03	0.82	38	4.84	1.28
38	4.89	0.91	50	5.10	1.35
48	5.73	0.96	60	5.13	1.37
59	6.44	1.04	100	5.03	1.33

[a] The data in the table are within ±0.05 deviation.

to the model, the time-dependent emission intensity of Py* can be represented by the following equation:

$$\frac{I(t)}{I(0)} = \frac{\int_{-\infty}^{\infty} \exp(x^2) \exp[-kt \exp(\gamma x)]\, dx}{\int_{-\infty}^{\infty} \exp(-x^2)\, dx} \quad (1)$$

where $\int_{-\infty}^{\infty} \exp(-x^2)\, dx = \pi^{1/2}$ and x is the integration range, and $I(0)$ is the initial emission intensity and $I(t)$ is the emission intensity at time t. The emission decay profile, as shown in Figure 4, is then characterized by a mean rate constant $\bar{k}_0$ and the width of the Gaussian distribution, γ, which reflects inhomogeneity of the system.

The Gaussian distribution characteristics of the emission decay of Py* in zeolites can be understood from the following facts: (a) any impurity in the samples may affect the pyrene photophysics although precautions were taken to eliminate this effect; (b) differences between the external and internal surfaces of zeolite; (c) differences in distribution of cations among channels; (d) differences in local electrostatic fields from cation to cation.[26] All of the effects (a), (b), (c), and (d) lead to a distribution of microenvironments for pyrene molecules, and to variations in the photophysics.

Fitting the curves in Figure 4 gives the values of $\bar{k}_{obs}$ and γ parameters, as shown in Table 2. The relationship between the observed decay rate constant, $\bar{k}_{obs}$, and pressure of oxygen is shown in the inserts of Figure 4, parts a and b, for zeolite L and mordenite, respectively, and for zeolite L the relationship can be described by

$$\bar{k}_{obs} = \bar{k}_0 + k'_q P_{O_2} \quad (2)$$

where P_{O_2} is the pressure of O_2, k'_q is the rate constant for quenching of Py* by O_2, and $\bar{k}_0$ is the mean decay rate constant in the absence of O_2. However, for mordenite, the relationship between the observed decay rate constant, $\bar{k}_{obs}$, and pressure of O_2 cannot be described by eq 2. The k'_q, obtained from eq 2 for Py–zeolite L, is 8.48 × 10^5 s^{-1} $mbar^{-1}$, which is consistent with the value obtained from steady-state fluorescence O_2-quenching studies (see above). Comparing the val-

(22) Albery, W. J.; Bartlett, P. N.; Wilde, C. P.; Darwent, J. R. *J. Am. Chem. Soc.* **1985**, *107*, 1854.
(23) (a) Draper, R. B.; Fox, M. A. *J. Phys. Chem.* **1990**, *94*, 4628. (b) Draper, R. B.; Fox, M. A. *Langmuir* **1990**, *6*, 1396.
(24) Liu, X.; Thomas, J. K. *Langmuir* **1993**, *9*, 727.
(25) Wolszczak, M.; Thomas, J. K. *Radiat. Phys. Chem.* **1991**, *38*, 154.
(26) (a) Dempsey, E. *J. Phys. Chem.* **1969**, *73*, 3660. (b) Dempsey, E. *Molecular Sieves*; Society of Chemical Industry: London, 1968; p 293.

ues obtained for Py–zeolites X and Y[12a] shows that the O_2-quenching rate constant of Py–zeolite L is about 1 order of magnitude smaller than those of Py–zeolites X and Y. This difference results from obstruction of the movement of O_2 in zeolite L, that is, due to the small size of the channel in zeolite L, 7.1 Å in diameter versus a 13 Å diameter for the supercage in zeolites X and Y.[1,27] The effect of the size of the channel on O_2 diffusion is even more severe in the case of mordenite where 30–35% pyrene molecules cannot be quenched. With these constraints, the pyrene molecules being quenched by O_2 are only those located at or near the boundary of the particles.

It is noted from Table 2 that the parameter γ for mordenite is bigger than that for zeolite L. This implies that although the channels of both zeolites are polar, the environment experienced by pyrene molecules in mordenite is more inhomogeneous compared to that in zeolite L. This can be understood on the basis of the following considerations: (1) the pyrene molecules in zeolite L may be randomly oriented and rotate about the axis of the channels due to the spherical character of the channels, which may average out the difference of environments experienced by pyrene molecules, while the pyrene molecules in mordenite can only orient toward the [010] direction (short axis of the channel[27]) and cannot rotate about the axis of the channels; (2) zeolite L has a lower Si/Al ratio (3.1) compared to that of mordenite (5.3), fluctuation of the surface charge should be small in zeolite L compared to in mordenite.

Table 2 also exhibits an increase of the parameter γ with increasing O_2 pressure. The change of γ with changing quencher concentration has been observed for systems such as silica,[16] alumina,[17] clays,[18] and anionic molecular assembly environments[25] and interpreted on the basis of interactions between the quencher and its surroundings.[25]

Fluorescence Anisotropy of Pyrene. To further understand the structural constraint of zeolites for pyrene, the fluorescence anisotropy of the excited pyrene in the zeolites L and M was measured, which provides information about the rotational movement of pyrene molecules in the system. The fluorescence anisotropy[28] (A) is defined as

$$A = \frac{I_{VV} - (I_{HV}/I_{HH})I_{VH}}{I_{VV} + 2(I_{HV}/I_{HH})I_{VH}} \qquad (3)$$

where I_{VV}, I_{HV}, I_{HH}, and I_{VH} represent the fluorescence intensity components measured vertically and horizontally with respect to the electric vector of the vertically and horizontally polarized excitation light. The ratio I_{HV}/I_{HH} is the instrumental correction factor which accounts for the intensity variation caused by the leakage of horizontally polarized light through the crossed polaroid. Experimentally, four fluorescence spectra were recorded under the conditions that the pair of polarizers was combined in either parallel or perpendicular ways. The fluorescence anisotropy of Py* in the zeolites was then calculated using the above equation. For comparison, the same is made for the Py–NaX sample.

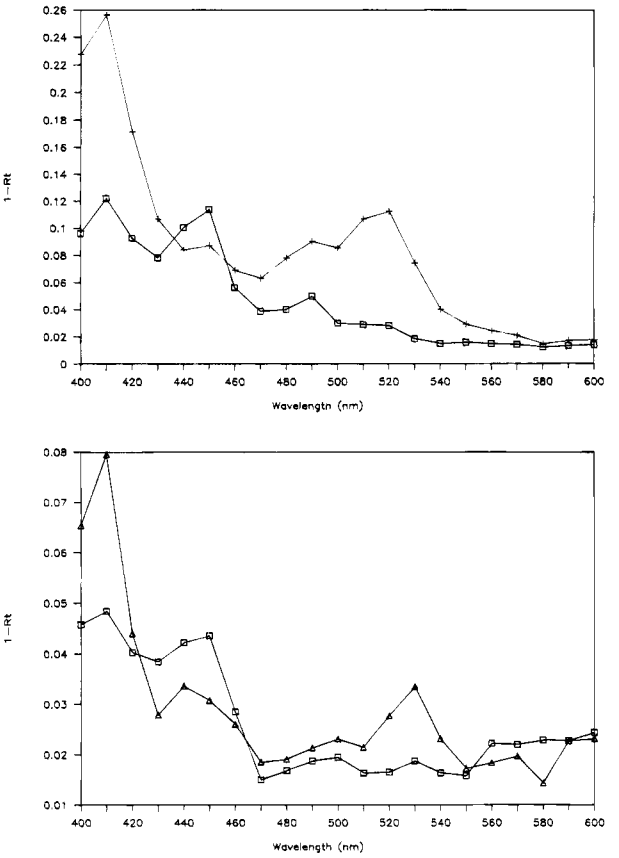

Figure 5. (a) Transient diffuse reflectance spectra of Py–zeolite L (symbol □ with line) and Py–Cs^+–zeolite L (symbol + with line). (b) Transient diffuse reflectance spectra of Py–mordenite (symbol □ with line) and Py–Cs^+–mordenite (symbol △ with line). Pyrene loading: 8×10^{-7} mol/g.

The results show that the values of fluorescence anisotropy of Py* in the zeolites M, L, and X are 0.102, 0.028, and −0.0031, respectively. It is clear from the results that the rotational movement of Py* is much easier in the zeolites with larger cavities or channels. The sequence of pyrene movement, PyX > PyL > PyM, observed is consistent with the sequence of the size of pores and channels of these zeolites. The tight fit of pyrene molecules in the channels of mordenite leads to the least rotational movement of the molecules, which is parallel with the results obtained from the O_2 quenching studies (see above).

Transient Species on Photolysis. Figure 5 gives the transient diffuse reflectance spectra of excited pyrene in zeolite L and mordenite. Three species of pyrene, triplet (^{3}py*), cation radical (py$^{\bullet+}$), and anion radical (py$^{\bullet-}$), with characteristic absorption bands at 410, 520, 450, and 490 nm,[16] respectively, were observed. The relatively weak absorption at the wavelength above 560 nm is possibly due to trapped electrons by Na^+ cation clusters as evidenced in the Na^+-zeolites X and Y.[12c–e] The pyrene triplet and cation radical have been observed in many systems such as Py–silica,[16] Py–alumina,[17] Py–clays,[18c] and Py–zeolites.[12c,e] The pyrene anion radical is readily formed in micelles and in solutions[29] but only recently has been observed in

(27) Meier, W. M.; Olson, D. H. *Atlas of zeolite structure types*; Butterworth: London, 1987.
(28) Azumi, T.; McGlynn, S. P. *J. Chem. Phys.* **1962**, *37*, 2413.
(29) (a) Katusin-Razem, B.; Wong, M.; Thomas, J. K. *J. Am. Chem. Soc.* **1978**, *100*, 1679. (b) Thomas, J. K.; Grieser, F.; Wong, M. *Ber. Bunsen-Ges. Phys. Chem.* **1978**, *82*, 937.

zeolites.[30] The surfaces of zeolite L and mordenite stabilize not only the pyrene cation radicals (electron transfer from the excited pyrene to the trapping sites of zeolite), but also the pyrene anion radicals (capture of electrons from the basic sites of the zeolites).[30] However, in these two zeolites, the yield of pyrene cation is much larger compared to that of pyrene anion radical, as seen in Figure 5. This characteristic is due to their intrinsic acidity and basicity, as demonstrated by studies for zeolites X and Y.[30] For zeolites L and mordenite, this is evidenced by studies of these zeolites with different basicities obtained by fine-tuning through Cs^+ ion exchange.[31] The yield of pyrene cation radical in these zeolites is decreased and that of pyrene anion radical increased for their more basic Cs^+ forms (see Figure 5). The increase in yield of pyrene triplet observed in the figure is due to the heavy atom effects, as proposed by Ramamurthy et al.[8]

(30) (a) Liu, X.; Iu, K.-K.; Thomas, J. K. *Chem. Phys. Lett.* **1993**, *204*, 163. (b) Liu, X.; Iu, K.-K.; Thomas, J. K. *J. Phys. Chem.* **1994**, *98*, 7877.

(31) (a) Barthomeuf, D. *Catalysis and Adsorption by Zeolites*; Ohlmann, G., Pfeifer, H., Fricke, R., Eds.; Elsevier Science Publishers B. V.: Amsterdam, 1991; p 157 and references therein. (b) Barthomeuf, D. *J. Phys. Chem.* **1984**, *88*, 42. (c) Besoukhanova, C.; Guidot, J.; Barthomeuf, D. *J. Chem. Soc., Faraday Trans. 1* **1981**, *77*, 1595.

Conclusion

Studies of adsorption and location of pyrene molecules in zeolites L and mordenite using photophysical techniques reveal that the internal surfaces of both zeolites are polar, similar to that observed for zeolites X and Y. The external surface of zeolite L is similar to its internal surface for adsorption of pyrene and excimers are easily produced on it, while the external surface of mordenite is different from its internal surface for adsorption and excimers are not observed on it even though a significant amount of pyrene is present in its supernatant. Due to the protection of pyrene molecules by the channels, the efficiency of O_2 quenching of the excited pyrene is 1 order of magnitude smaller in zeolite L than in zeolite X and Y,[12a] and 30−35% of pyrene cannot be quenched by O_2 in mordenite. The rotational movement of pyrene in the zeolites is restricted by the structure as revealed by the fluorescence anisotropy measurements. Photolysis studies reveal that both cation and anion radicals can form in the zeolites with preference of pyrene cation radicals.

Acknowledgment. The authors thank NSF for the financial support of this work.